Featured-Based Registration of Terrestrial Laser Scans with Minimum Overlap Using Photogrammetric Data

Erwan Renaudin, Ayman Habib, and Ana Paula Kersting

Currently, there is a considerable interest in 3D object reconstruction using terrestrial laser scanner (TLS) systems due to their ability to automatically generate a considerable amount of points in a very short time. To fully map an object, multiple scans are captured. The different scans need to be registered with the help of the point cloud in the overlap regions. To guarantee reliable registration, the scans should have large overlap ratio with good geometry for the estimation of the transformation parameters among these scans. The objective of this paper is to propose a registration method that relaxes/eliminates the overlap requirement through the utilization of photogrammetrically reconstructed features. More specifically, a point-based procedure, which utilizes non-conjugate points along corresponding linear features from photogrammetric and TLS data, will be used for the registration. The non-correspondence of the selected points along the linear features is compensated for by artificially modifying their weight matrices. The paper presents experimental results from simulated and real datasets to illustrate the feasibility of the proposed procedure.

Keywords: Close range photogrammetry, point cloud, segmentation, linear features, terrestrial laser scanner.

Manuscript received Dec. 17, 2010; revised June 7, 2011; accepted July 1, 2011.

This work was supported by the GEOmatics for Informed Decisions (GEOIDE) NCE network and Natural Sciences and Engineering Research Council of Canada (NSERC) Discovery and Strategic Project Grants.

Erwan Renaudin (phone: +1 403 220 3034, email: erwan.renaudin@ucalgary.ca), Ayman Habib (email: ahabib@ucalgary.ca), and Ana Paula Kersting (email: ana.kersting@ucalgary.ca) are with the Digital Photogrammetry Research Group, Department of Geomatic Engineering, University of Calgary, Alberta, Canada.

doi:10.4218/etrij.11.1610.0006

I. Introduction

Current technologies for accurate 3D object reconstruction include digital photogrammetric and terrestrial laser scanner (TLS) systems. The photogrammetric reconstruction process is based on redundant measurements in which an over-determined system of equations is manipulated in a least squares adjustment (LSA) procedure to derive the ground coordinates of the imaged object points [1]. The major shortcoming of this technique is the complicated and sometimes unreliable automated matching procedures. For instance, when dealing with large-scale imagery, automatic matching procedures are not reliable and manual editing is necessary. In contrast to photogrammetry, the TLS point reconstruction is based on non-redundant measurements; that is, the number of equations is equivalent to the number of unknown ground coordinates. Moreover, TLS data is mainly of a positional nature compared to the positional and spectral information in imagery, which leads to better thematic interpretation of photogrammetric data. The main advantage of TLS systems is the direct acquisition of a high-density 3D point cloud. A TLS system measures distances to points on the object illuminated by the laser at uniform increments in the horizontal and vertical directions. These measurements are then converted into a Cartesian coordinate system, mostly a local system associated with the scanner. Since the TLS remains static while collecting the data, multiple scans are frequently required in order to model the whole object. In this regard, appropriate methods for registering the data from the different scanning locations to a common reference frame should be implemented.

Most of the available commercial software packages for TLS data registration (for example, INUS Rapidform, Leica

Cyclone, and Trimble's INPHO) are based on the iterative closest point (ICP) algorithm [2], which is based on minimizing the inter-point distances between two overlapping surfaces. Although the ICP is an acceptable procedure for the registration of surfaces represented by irregularly distributed points, the utilization of such algorithm requires a large overlap ratio with appropriate geometry among the involved datasets. These requirements are not exclusive to the ICP procedure but valid for any registration method based on the use of the TLS point cloud only [3]. In this regard, registration methods that combine datasets from different sources have been investigated in the past few years.

Another approach for TLS data registration is based on the utilization of photogrammetric data as well as surveyed distinct points. For example, Fabris and others [4] proposed a semi-automated correlation-based image matching algorithm for 3D point extraction from the photogrammetric dataset. The ground coordinates of some of the matched points are then surveyed with a total station. The surveyed points, matched image points, and identified corresponding points in the laser data are used for the coregistration of the TLS and the photogrammetric datasets to the reference frame defined by the surveyed points. The drawback of this approach is the use of point primitives, which are not easily identifiable in the TLS data. Also, this approach requires some effort for surveying the control points.

Another solution for TLS data registration using photogrammetric data is presented in [5]. This approach is based on having the laser scanner and the digital camera rigidly fixed together on a single mount during the acquisition process. The spatial and rotational offsets between the laser scanner and the camera are determined through a calibration process, which is based on a single photo resection using distinct points that have been measured by the scanner and could be identified in the image. A minimum of three points is necessary for this calibration process. After the calibration, the spatial and the rotational offsets are assumed to be constant, and the system can be used for data collection around objects of interest. After the data collection, a relative orientation between acquired images can be performed to determine the exterior orientation parameters (EOPs) relative to an arbitrary reference frame. Then, the images' EOP can be transferred to the TLS stations using the estimated spatial and rotational offsets from the calibration procedure. The drawback of this approach, from an operational point of view, is that mounting the digital camera on the TLS unit is not always appropriate since a good observation station for TLS data collection is not necessarily a good one for collecting the images. The authors in [6] proposed an innovative approach that combines datasets from different sources in which an interactive orientation method is utilized to register aerial and terrestrial images with airborne LiDAR data. Although airborne LiDAR is utilized in the work, the presented method can also be used for registering TLS data. The shortcoming of this method is that it involves manual steps which are critical and highly operator-dependent.

Other authors proposed methods for the coregistration of the TLS and photogrammetric data while assuming that the TLS scans have been already registered [7], [8]. The main purpose of these methods was the integration of the TLS and the photogrammetric data to explore their complementary nature. In [7], linear features extracted from the TLS point cloud are used as control lines in the bundle adjustment procedure. In [8], the TLS data is used to improve the photogrammetric matching process for the extraction of building break lines (edges). The complementary nature of laser and photogrammetric data has been highlighted by several other authors [9]-[12].

The objective of this paper is to propose an effective registration procedure for the coalignment of the TLS scans with minimal overlap. For that purpose, the utilization of photogrammetric data is investigated while circumventing the limitations of existing approaches in [5], [6]. More specifically, the proposed method does not require the TLS and the camera to be mounted together during the data collection and is not highly operator-dependent. Moreover, appropriate primitives, which can be reliably extracted from the TLS and photogrammetric data, are introduced. Rather than using conjugate points [4], linear features are utilized in this research work. Besides the registration of the TLS scans to a common reference frame, the proposed method will also ensure the coregistration of the photogrammetric and TLS data as a byproduct, which will have a positive impact on further products such as the generation of photo-realistic 3D models.

In section II, a detailed description of the proposed method is presented. In section III, the performance and feasibility of the proposed methodology is evaluated through experimental results from simulated and real datasets. Finally, the paper presents some conclusions and recommendations for future work in section IV.

II. Proposed Methodology

In this section, the proposed methodology for the registration of the TLS scans is described. An effective registration process should deal with three main issues: the transformation function relating the reference frames of the involved datasets, the registration primitives, and the similarity measure which utilizes conjugate primitives for the estimation of the involved parameters in the transformation function [13]. As already mentioned, the utilization of terrestrial laser point cloud only in the registration process would demand large overlap ratio between adjacent scans with suitable geometry to allow for a

reliable estimation of the transformation parameters. Hence, an effective registration method is introduced while relaxing/eliminating the overlap requirement through the utilization of photogrammetrically reconstructed features. These features will ensure reliable estimation of the transformation parameters relating the different laser scans' reference frames and the global reference frame. The photogrammetrically reconstructed features will guarantee strong tying between the different laser scans and the reference one as long as appropriate geometry is available between each of the laser scans and the photogrammetric model.

In the absence of systematic errors, a six-parameter rigid-body transformation with three translations and three rotations will ensure the coalignment of the different laser scans since the TLS measurements provide true scale. On the other hand, the coalignment of the photogrammetrically reconstructed features to the common reference frame will require a 3D similarity transformation (three translations, three rotations, and a scale factor).

Traditionally, photogrammetric registration procedures are usually based on point primitives. These primitives, however, are not suitable when dealing with laser scan data since it is quite difficult to establish the correspondence between distinct points in the irregularly-distributed datasets. In this regard, the use of linear features is proposed. In the following subsections, the primitive extraction procedure for the photogrammetric and laser datasets will be described. Also, the similarity measure, which incorporates the extracted primitives for the estimation of the parameters of the transformation function, will be presented.

1. Primitives Extraction

As mentioned earlier, the use of point primitives when dealing with laser scan data is not appropriate unless a probabilistic approach is utilized. Therefore, linear features are employed instead. The motivation behind the utilization of these primitives is that man-made objects are rich in linear features, making their use appropriate for several applications, such as virtual city visualization, building reconstruction, and road network mapping. Moreover, such primitives can be reliably extracted from both datasets as will be explained in this subsection. One should note that the reliability of the primitive extraction is related to the practicality of deriving these features while considering the nature of the TLS and photogrammetric data.

The incorporation of linear features in the photogrammetric triangulation procedure is performed using the coplanarity-based method presented in [14], [15], where the object space straight lines are represented by two points along the line while

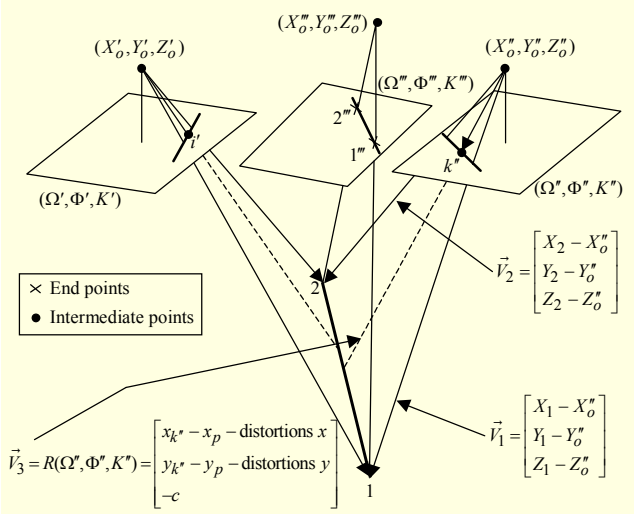

Fig. 1. Perspective transformation between image and objectspace straight lines and coplanarity constraint for intermediate points along the line.

image space lines are represented by a sequence of 2D coordinates of intermediate points along the feature. The measurement of tie lines appearing in a group of overlapping images starts by identifying its end points in one or two images along the line under consideration. These end points are used to define the corresponding object space line segment, which are estimated in the bundle adjustment procedure. It is worth mentioning that these points need not be identifiable or even visible in other images. The relationship between the image coordinates of the line end points $\{(x_1, y_1), (x_2, y_2)\}$ and the corresponding ground coordinates $\{(X_1, Y_1, Z_1), (X_2, Y_2, Z_2)\}$ is established through the collinearity equations. Then, intermediate points along the line are measured in all overlapping images. One should note that these points are monoscopically selected; that is, they need not be conjugate points. The intermediate points are included into the adjustment procedure through the coplanarity constraint shown in

$$(\vec{V}_1 \times \vec{V}_2) \cdot \vec{V}_3 = 0. \quad (1)$$

In this equation, $\vec{V}_1$ is the vector connecting the perspective center to the first end point along the object space line, $\vec{V}_2$ is the vector connecting the perspective center to the second end point along the object space line, and $\vec{V}_3$ is the vector connecting the perspective center to an intermediate point along the corresponding image line (Fig. 1). The constraint in (1) can be introduced for all the intermediate points (for example, i' and k'' in Fig. 1) along image space linear features. One should note that the coplanarity constraint does not introduce any new unknowns to the adjustment procedure.

In this work, the bundle adjustment is performed using an arbitrary reference frame. More specifically, seven parameters

are arbitrarily fixed to define the datum. The seven parameters can be either associated with the EOP of the imagery or the ground coordinates of tie points. The outcome of such a procedure is a set of 3D linear features defined relative to an arbitrary reference frame. These linear features are defined by two points along the line.

To extract linear features from the laser scans, a semi-automated approach was employed. The process starts by displaying the irregularly-distributed point cloud and selecting areas where linear features might exist. Then, an automated segmentation technique is adopted to identify the best-fitting planar patches in the selected areas through the minimization of the normal distances between the segmented patches and the point cloud. The outcome from such segmentation is aggregated sets of points representing planar patches in the selected area along with their best fit planes. For the extraction of the linear features, neighboring planar patches are identified and intersected to produce straight-line segments. Similar to the photogrammetric features, the TLS lines will be represented by two points along each line. This procedure is repeated for all the laser scans to extract all lines which are conjugate to the photogrammetrically reconstructed linear features. The matching of the lines extracted from the laser scans and the photogrammetrically derived ones is established manually by the operator. One should note that this is a straight forward process and does not require an experienced operator.

2. Similarity Measure

In this subsection, the similarity measure, which incorporates the matched primitives together with the transformation function to mathematically describe their correspondence, is introduced. The formulation of the similarity measure depends on the representation scheme for the involved primitives. In this work, the linear features are represented by its end points. Assuming that the end points representing corresponding linear features are conjugate to each other, the mathematical model, based on a 3D similarity transformation function relating the observed coordinates of these points in the laser scans and the photogrammetrically reconstructed data $\vec{X}_{\mathrm{TLS}_i/\mathrm{Pho}}$ to the global ground coordinates $\vec{X}_{\mathrm{G}}$, would get the form in

$$\vec{X}_{\mathrm{TLS}_i/\mathrm{Pho}} = \vec{X}_{T_{\mathrm{TLS}_i}/\mathrm{Pho}} + S_{\mathrm{TLS}_i/\mathrm{Pho}} R_{\mathrm{TLS}_i/\mathrm{Pho}} \vec{X}_{\mathrm{G}}, \quad (2)$$

where *i* indicates the *i*-th scan. This mathematical relationship can be represented by the traditional Gauss Markov stochastic model in

$$\vec{y} = A\vec{x} + \vec{e} \qquad \vec{e} \sim (0, \Sigma), \qquad \Sigma = \sigma_o^2 P^{-1}, \quad (3)$$

where $\vec{y}$ is the *nx*1 vector of observations ($\vec{X}_{\mathrm{TLS}_i/\mathrm{Pho}}$); $\vec{x}$ is the *mx*1 vector of unknowns: $\vec{X}_{T_{\mathrm{TLS}_i/\mathrm{Pho}}}$ (three shifts), $S_{\mathrm{TLS}_i/\mathrm{Pho}}$ (one scale factor), $(\omega, \varphi, \kappa)_{\mathrm{TLS}_i/\mathrm{Pho}}$ (three rotation angles defining the rotation matrix $R_{\mathrm{TLS}_i/\mathrm{Pho}}$), and $\vec{X}_{\mathrm{G}}$ (the global coordinates); considering the transformation parameters for *ns* scans, the transformation parameters for the photogrammetric model, and the ground coordinates of *nt* tie points, the number of unknown parameters will be equal to 7**ns*+7+3**nt*; *A* is the *nxm* design matrix; and $\vec{e}$ is the *nx*1 vector of random noise, which is normally distributed with a zero mean and variance-covariance matrix Σ that is obtained by the product of the a priori variance factor σ_o^2 and the weight matrix *P*. The LSA procedure aims at estimating the unknown parameters which minimize the sum of squares of weighted residuals in (4) and leads to the solution vector in (5), the predicted residuals in (6), the variance-covariance matrix in (7), and the a posteriori variance factor in (8) [16]:

$$\vec{e}^T P \vec{e} = \min\big|_{\vec{x}}, \quad (4)$$

$$\hat{\vec{x}} = (A^T PA)^{-1} A^T P\vec{y} = N^{-1} A^T P\vec{y}, \quad (5)$$

$$\hat{\vec{e}} = \vec{y} - A\hat{\vec{x}}, \quad (6)$$

$$\Sigma\{\hat{\vec{x}}\} = \hat{\sigma}_o^2 (A^T PA)^{-1} = \hat{\sigma}_o^2 N^{-1}, \quad (7)$$

$$\hat{\sigma}_o^2 = (\hat{\vec{e}}^T P\hat{\vec{e}}) / (n-m). \quad (8)$$

Due to the nature of the linear feature extraction procedure from the laser scans and the photogrammetric data, one can note that the definition of the line end points is quite arbitrary. As a result, the points representing corresponding linear features from the laser scans and the photogrammetric data are not necessarily conjugate to each other. Therefore, the abovementioned LSA solution cannot be directly used to come up with an estimate for the unknown parameters.

Starting from (2), the mathematical model describing the relationship between the observed coordinates of non-conjugate points along correspondent linear features in the laser scans/photogrammetrically reconstructed data and the global ground coordinates will take the form in (9), which can be represented by the Gauss Markov stochastic model in (10):

$$\vec{X}_{\mathrm{TLS}_i/\mathrm{Pho}} = \vec{X}_{T_{\mathrm{TLS}_i}/\mathrm{Pho}} + S_{\mathrm{TLS}_i/\mathrm{Pho}} R_{\mathrm{TLS}_i/\mathrm{Pho}} \vec{X}_{\mathrm{G}} + d\vec{X}, \quad (9)$$

$$\vec{y} = A\vec{x} + d\vec{X} + \vec{e} \quad \vec{e} \sim (0, \Sigma). \quad (10)$$

The difference between this model and the one in (3) is the additional unknown vector $d\vec{X}$ resulting from using non-conjugate points (Fig. 2). It should be noted that the additional vector of unknowns $d\vec{X}$ is defined along the linear feature under consideration; that is, only the component of this vector

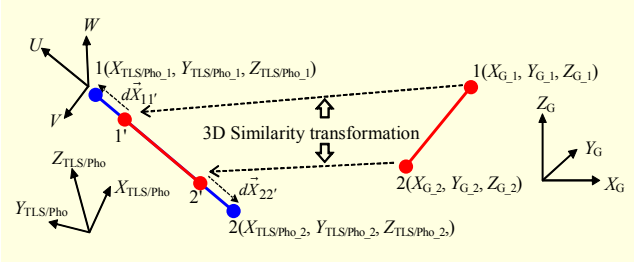

Fig. 2. Mathematical model, that is, a 3D similarity transformation, relating lines defined relative to global coordinate system to lines defined relative to the scans/photogrammetric coordinate system along with additional unknown vector $d\vec{X}$ which is defined along the linear feature.

along the line is different from zero.

The question now is how to modify the LSA to deal with the model in (10) while eliminating the unknown vector $d\vec{X}$ from the parameters to be estimated. To explain the proposed modification process, we will start by changing the stochastic properties of the random noise vector as represented by

$$\Sigma`\{\vec{e}\} = \sigma_o^2 P`^{+}, \quad P`d\vec{X} = 0. \tag{11}$$

The new weight matrix $P`$ of the noise vector is chosen such that $P`d\vec{X} = 0$; that is, the unknown vector $d\vec{X}$ belongs to the null space of the weight matrix $P`$. Such a condition signifies that the modified weight matrix is not positive-definite; that is, the inverse matrix $P`^{-1}$ does not exist. Therefore, the modified variance-covariance matrix will be represented as $\Sigma`\{\vec{e}\} = \sigma_o^2 P`^{+}$, where the plus sign indicates the Moore-Penrose pseudoinverse. Starting from the modified variance-covariance/weight matrix and the LSA principles, the solution will be derived in the following sequence of equations.

Using the modified weight matrix, the LSA target function can be redefined as in (12), which can be reduced to the form in (13). Thus, the solution vector ($\hat{\vec{x}}$) to the LSA target function is defined as shown in (14). Using the law of error propagation, the variance-covariance matrix of the solution vector, $\Sigma\{\hat{\vec{x}}\}$, can be obtained as presented in (15):

$$\vec{e}^T P`\vec{e} = (\vec{y} - A\vec{x} - d\vec{X})^T P`(\vec{y} - A\vec{x} - d\vec{X}) = \min\Big|_{\vec{x}, d\vec{X}}, \tag{12}$$

$$\vec{e}^T P`\vec{e} = (\vec{y} - A\vec{x})^T P`(\vec{y} - A\vec{x}) = \min\Big|_{\vec{x}}, \tag{13}$$

$$\hat{\vec{x}} = (A^T P`A)^{-1} A^T P`\vec{y} = N^{-1} A^T P`\vec{y}, \tag{14}$$

$$\Sigma\{\hat{\vec{x}}\} = \sigma_o^2 N^{-1}. \tag{15}$$

The last step is to estimate the a posteriori variance factor ($\hat{\sigma}_o^2$) by deriving the expected value of the sum of squares of weighted predicted residuals. Starting from (16), one can derive an estimate for the a posteriori variance factor according to (17), where q is the rank of the modified weight matrix $P`$:

$$\begin{aligned} E(\vec{\tilde{e}}^T P`\vec{e}) &= E\{(\vec{y} - A\hat{\vec{x}} - d\vec{X})^T P`(\vec{y} - A\hat{\vec{x}} - d\vec{X})\} \\ &= E\{(\vec{y} - A\hat{\vec{x}})^T P`(\vec{y} - A\hat{\vec{x}})\} = (q-m)\sigma_o^2, \end{aligned} \tag{16}$$

$$\hat{\sigma}_o^2 = (\vec{y} - A\hat{x})^T P`(\vec{y} - A\hat{x})(q-m). \tag{17}$$

In summary, from an implementation point of view, the LSA solution to the stochastic model in (18) can be derived using (14), (15), and (17):

$$\vec{y} = A\vec{x} + d\vec{X} + \vec{e} \quad \vec{e} \sim (0, \Sigma`), \tag{18}$$

where $\Sigma` = \sigma_o^2 P`^{+}$ and $P`d\vec{X} = 0$. This solution is similar to the solution of the traditional Gauss Markov model (5)-(8) with the exception that the redundancy is evaluated as the difference between the rank of the modified weight matrix and the number of unknowns. Thus, the modification in the weights of the noise vector allows for the elimination of the additional unknown vector $d\vec{X}$ while having almost no impact on the traditional LSA.

So far, we established that by modifying the weight matrix to satisfy the condition in (11), one can derive an estimate of the unknown parameters while dealing with non-conjugate points along corresponding linear features. Now we need to derive the modified weight matrix $P`$. This can be established according to the following procedure. First, we define a local coordinate system (UVW) with the U axis aligned along the line in question. Note that the definitions of the V and W axes are arbitrary. With the manipulation of the weight matrix, the LSA target function minimizes the weighted sum of the squared distances along the normal from the end points of one linear feature to the correspondent one. Having said that, different definitions for V and W will just define different components for the vector, whose magnitude will be minimized in the LSA procedure. The relationship between the laser scans/photogrammetrically derived data coordinate systems $(XYZ)_{TLS/Pho}$ and the local coordinate system (UVW) can be represented by (19). The rotation matrix (M) in that equation is obtained using the components of the unit vectors, U, V, and W defined relative to the $(XYZ)_{TLS/Pho}$ system. The original weight matrix P_{XYZ}, as shown in (20), is defined by the inverse of the variance-covariance matrix Σ_{XYZ}, which depends on the linear feature extraction procedure. More specifically, for the laser scan linear features, it will be based on the plane fitting/intersection precision while for the photogrammetric linear features, it will be based on the variance-covariance matrix of the estimated lines' end points in the photogrammetric bundle adjustment. Using the law of error propagation, the weight of that point in the local coordinate

system P_{UVW} can be derived according to (21). This weight matrix can be modified according to (22). Finally, the modified weight matrix $P`_{XYZ}$ in the laser scans/photogrammetric data coordinate systems can be derived according to (23):

$$\begin{bmatrix} U \\ V \\ W \end{bmatrix} = M \begin{bmatrix} X \\ Y \\ Z \end{bmatrix} = \begin{bmatrix} U_x & U_y & U_z \\ V_x & V_y & V_z \\ W_x & W_y & W_z \end{bmatrix} \begin{bmatrix} X \\ Y \\ Z \end{bmatrix}, \tag{19}$$

$$P_{XYZ} = \Sigma_{XYZ}^{-1}, \tag{20}$$

$$P_{UVW} = MP_{XYZ}M^T = \begin{bmatrix} P_U & P_{UV} & P_{UW} \\ P_{VU} & P_V & P_{VW} \\ P_{WU} & P_{WV} & P_W \end{bmatrix}, \tag{21}$$

$$P`_{UVW} = \begin{bmatrix} 0 & 0 & 0 \\ 0 & P_V & P_{VW} \\ 0 & P_{WV} & P_W \end{bmatrix}, \tag{22}$$

$$P`_{XYZ} = M^T P`_{UVW} M. \tag{23}$$

Using the established procedure for the weight modification, (24) demonstrates that $P`_{XYZ} = d\vec{X}$ equals zero, while noting that the vector $d\vec{X}$ is aligned along the linear feature. In (24), dX, dY, and dZ represent the components of the $d\vec{X}$ vector w.r.t. the $(XYZ)_{\text{TLS/Pho}}$ system, while dU, dV, and dW are the components of the $d\vec{X}$ vector w.r.t. the (UVW) system, and therefore dV and dW will equal to zero.

$$\begin{aligned} P`_{XYZ}\, d\vec{X} &= M^T P`_{UVW} M d\vec{X} = M^T P`_{UVW}\, d\vec{U} \\ &= M^T \begin{bmatrix} 0 & 0 & 0 \\ 0 & P_V & P_{VW} \\ 0 & P_{WV} & P_W \end{bmatrix} \begin{bmatrix} dU \\ 0 \\ 0 \end{bmatrix} = 0. \end{aligned} \tag{24}$$

In summary, the proposed registration procedure proceeds as follows:

Step 1. Linear features are extracted from the laser scans and the photogrammetric data using the procedures described in subsection II.1. Corresponding linear features are represented by their end points, which might not be conjugate. The points representing corresponding linear features will be assigned the same identification code.

Step 2. For each of the points representing the extracted features, one can write the observation equations similar to those in (2). For the TLS, the scans' scale factor can be fixed to unity since the TLS measurement process provides true scale. To compensate for the fact that the utilized points along corresponding lines are not conjugate, their weights should be modified. The weight modification should be carried out for all the points sharing the same identification code except one. The point without weight modification will be used to define the adjusted ground global coordinates of that point along the feature in question. Maintaining the weight for that point is necessary since the weight modification process only controls the point position in the normal direction to the enclosing feature.

Step 3. The transformation parameters for the individual scans and the photogrammetrically reconstructed data as well as the coordinates of the observed features in the global coordinate system are determined through a LSA procedure. During such an adjustment procedure, the individual scans and the photogrammetrically reconstructed data are independently rotated, shifted, and scaled until they fit together as well as possible. The global coordinate system for the registration procedure can be established by using one of the scans as a reference frame. In other words, the individual scans and the photogrammetrically reconstructed data will be rotated, shifted, and scaled until they are compatible with each other and fit with the reference scan as well as possible.

Step 4. The estimated transformation parameters are applied to the respective scans using (25) to obtain the coordinates of all points in the global coordinate system:

$$\vec{X}_{\text{G}} = -\frac{1}{S_{\text{TLS}_i}} R^T_{\text{TLS}_i} (\vec{X}_{T_{\text{TLS}_i}} - \vec{X}_{\text{TLS}_i}). \tag{25}$$

Note that a minimum of two corresponding non-coplanar lines should be common between each of the laser scans and the photogrammetric model for the estimation of the transformation parameters since a line-pair has four degrees of freedom which contribute towards the estimation of the 3D-similarity transformation between these models [14].

III. Experimental Results

1. Simulated Dataset

The main purpose of utilizing synthetic data for the experiments is to verify the performance of the proposed registration procedure using the scans only and the scans together with the photogrammetrically-derived model in a controlled environment. The simulated object along with the simulated scans configuration is illustrated in Fig. 3. The simulated Gaussian noise in the generated lines is 10 cm at one sigma. Table 1 presents the simulated transformation parameters, which are defined in (2). Note that scan 2 was taken as the reference frame in the experiments.

In Fig. 3, the geometry of conjugate lines in the scans' overlapping areas is very weak since we have only two parallel lines that are common among each scan pair. More specifically, overlapping scans can slide along the lines' direction while

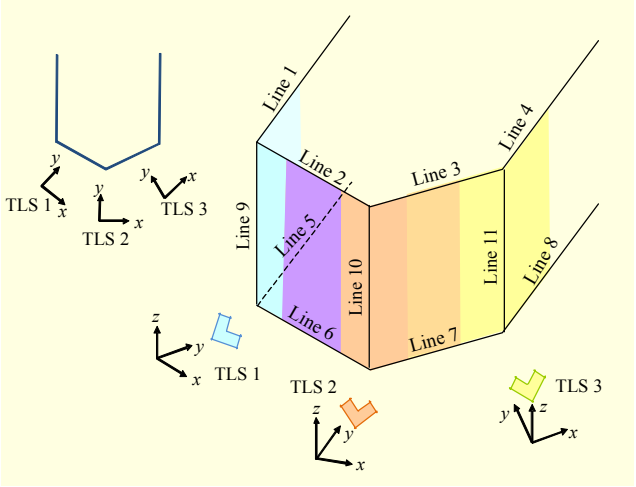

Fig. 3. Simulated object along with scans configuration.

Table 1. Simulated transformation parameters.

	X_T (m)	Y_T (m)	Z_T (m)	S	ω(°)	ϕ(°)	κ(°)
Scan 1	–8.00	–3.00	0.50	1.000	0.5000	1.0000	45.000
Scan 3	7.50	3.00	0.10	1.000	0.5000	0.1000	–43.000
Photo	1.00	–5.00	0.50	0.800	2.0000	1.5000	–10.000

Table 2. Estimated transformation parameters from simulatedTLS scans and photogrammetric model.

	X_T (m±m)	Y_T (m±m)	Z_T (m±m)	S	ω (°±°)	φ (°±°)	κ (°±°)
Scan 1	–7.65 ±0.17	3.33 ±0.15	0.55 ±0.11	1.000	0.7811 ±0.3478	0.6382 ±0.4559	46.4120 ±0.6170
Scan 3	7.57 ±0.19	2.81 ±0.18	0.14 ±0.13	1.000	0.7686 ±0.3624	0.5201 ±0.5067	–41.7490 ±0.7168
Photo	1.06 ±0.11	–5.11 ±0.08	0.62 ±0.08	0.7975 ±0.0030	1.5059 ±0.3546	1.4065 ±0.3036	–9.6819 ±0.4916

maintaining the collinearity of conjugate linear features. Therefore, singularity is expected in the adjustment procedure when trying to estimate the transformation parameters relating those scans. The experiments carried out using the simulated data have confirmed such findings.

The singularity encountered when using the TLS scans only in the registration procedure can be overcome by the inclusion of a photogrammetric model, which encompasses all the eleven lines shown in Fig. 3. The geometry of conjugate lines from each scan and the photogrammetric model allows for a reliable estimation of the transformation parameters. In other words, each of the scans has more than two non-coplanar lines that are available in the photogrammetric model. This expectation is validated through the experimental results whose transformation parameters are reported in Table 2.

Table 3. Quantitative comparison between simulated and estimated transformation parameters through RMSE analysis.

		Scan 1 estimated vs. simulated	Scan 3 estimated vs. simulated	Photo estimated vs. simulated
RMSE (m)	X	0.10 (0.04±0.09)	0.11 (0.09±0.07)	0.04 (0.02±0.03)
(Mean±Std)	Y	0.15 (0.13±0.08)	0.07 (–0.04±0.06)	0.08 (0.07±0.05)
(m±m)	Z	0.03 (0.00±0.03)	0.04 (0.02±0.03)	0.04 (0.01±0.04)

To verify the equivalency between the estimated and the simulated transformation parameters, one can compare the numerical values of the individual parameters. Comparing the numerical values in Tables 2 and 3, one can see that estimated shifts seem to be close to the true ones. However, it seems that there are significant differences in the angular values. However, such a procedure would not consider possible correlations among the estimated parameters. Moreover, it would not lead to a meaningful quantitative measure of the equivalency or deviation. Therefore, a meaningful comparison should be based on evaluating the impact of the deviation between the estimated and true parameters on the transformed point clouds using both sets of parameters. Similar to [17], a gridded volume is utilized for quantitative comparison of the estimated and true transformation parameters. It should be noted that the gridded volume is generated using the same planimetric and vertical extent of the volume covered by each scan. The vertices of the gridded volume are then transformed using the two sets of transformation parameters, the estimated and the simulated ones. The coordinates of conjugate vertices, following the application of the transformation parameters, are compared through an RMSE analysis. If the estimated RMSE values are within the estimated noise level in the point cloud (in this work, a noise level of ±10 cm was simulated), the estimated transformation parameters are deemed equivalent. The RMSE values presented in Table 3 are compatible with the data noise level, thus indicating the equivalency between the simulated and estimated transformation parameters in Tables 1 and 2, respectively. Based on such analysis, one can conclude that the angular deviation is not significant. Therefore, the quality of the angular deviation and its standard deviation should be considered in the context of the data extent in the direction of the rotation axis as well as the noise level in the point cloud.

2. Real Dataset

After verifying the feasibility and performance of the proposed procedure using simulated data, a real dataset was acquired to test the performance of the method using data from

operational systems. For that purpose, a terrestrial laser survey was carried out using a Trimble Terrestrial Laser Scanner (GS200) with maximum range of 200 m and resolution up to 32 milliradians (or 3 mm at 100 m). The data was captured over a building, which is shown in Fig. 4. This building was selected due to its architecture, which represents well the facades typically mapped in urban environments.

In order to cover the whole building facade, three scans were acquired from three locations with an average sampling distance of 2 cm. Figure 5 illustrates the acquired scans. The settings of the scanner were chosen in order to have two averaged distance measurements for each point derived by the scanner. The distance of acquisition ranged roughly from 50 m to 90 m. Several gaps were observed in the laser scanning data due to the glass reflective material superimposed on the building facades and especially over the windows that were transparent for the wavelength of the scanner. Thus, no returned echoes were observed from these portions of the building and were therefore missing in the final model.

The collection of the photogrammetric dataset was performed using a Canon EOS Rebel XT digital single lens reflex camera. The utilized camera has an array dimension of 3456×2304 pixels and a nominal focal length of 35 mm. In order to determine the internal characteristics of the camera, a calibration procedure was carried out. An outdoor calibration test field was used for that purpose. The utilized test field includes several targets that were previously surveyed with a total station. These targets were used as ground control points in the self-calibration procedure. Also, additional tie points for enhancing the global geometry and constraining the photogrammetric process were added in the calibration. A total of five convergent images were taken over the building.

Before applying the proposed methodology, the registration between the three laser scans was attempted using a commercial software package, which is based on the ICP algorithm. Since the ICP algorithm requires good approximate values, manual detection of tie points were introduced to initiate the registration process between the three different point

(a) (b)

Fig. 4. (a) Trimble/Mensi GS200 and (b) surveyed building.

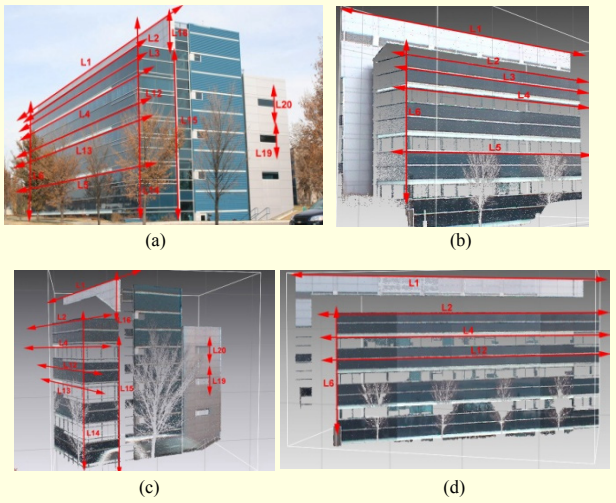

(a) (b) (c) (d)

Fig. 5. Image illustrating surveyed building: (a) with photogrammetrically reconstructed linear features, (b) extracted from TLS scan 1, (c) scan 2, and (d) scan 3.

clouds. However, due to the poor geometry between the scans (see Fig. 5), high correlations between the parameters were observed between scans 1 and 2. Moreover, between scans 2 and 3, the software was not able to compute any transformation parameters. This might be attributed to the fact that conjugate surface elements are composed of two parallel planar surfaces, thus not allowing for full recovery of the transformation parameters. Such limitations are expected to be overcome by the utilization of the proposed methodology.

First, the proposed semi-automated procedure for the extraction of corresponding linear features in the laser scans and the photogrammetric data, described in subsection II.1, was applied. A total of thirteen lines were photogrammetrically derived, which are illustrated in Figure 5(a). Plane intersection for the derivation of the TLS lines was mainly achieved through the cornices present in the scans. In some cases, where the intersection was not possible to achieve, we manually selected a number of points to compute the best fitting line. For instance, along the upper edge of the building, a mean of the highest elevation points recorded was computed to define the elevation of the horizontal line. To avoid any confusion and systematic errors in the adjustment, those particular lines had to be monitored closely in terms of residuals. A total of twenty-one lines were collected over the three scans (six lines in scan 1, five lines in scan 2, and ten lines in scan 3). The extracted lines from the terrestrial laser scans are illustrated in Figs. 5(b) to (d). Note in Fig. 5 that each scan has more than two non-coplanar lines which are available in the photogrammetric data.

Following the extraction of the involved primitives, the registration transformation parameters are estimated. To demonstrate the limitation of using TLS scans only,

Table 4. Real data results using TLS scans 1 and 2 only.

	X_T (m±m)	Y_T (m±m)	Z_T (m±m)	S	ω (°±°)	ϕ (°±°)	κ (°±°)
Scan 2	–25.86 ±0.11	–16.13 ±0.05	0.23 ±0.16	1.000	0.2109 ±0.1954	0.8066 ±0.1955	43.2910 ±0.1424

Table 5. Estimated transformation parameters using TLS data and photogrammetric model.

	X_T (m±m)	Y_T (m±m)	Z_T (m±m)	S	ω (°±°)	ϕ (°±°)	κ (°±°)
Scan 2	–25.81 ±0.09	–16.16 ±0.06	0.30 ±0.20	1.000	0.1225 ±0.2379	0.6960 ±0.1931	43.3217 ±0.0969
Scan 3	–43.48 ±0.07	82.35 ±0.13	0.12 ±0.18	1.000	0.1257 ±0.1482	–0.3353 ±0.2406	–57.9702 ±0.1038
Photo	6.67 ±0.07	71.66 ±0.08	22.78 ±0.14	0.8821 ±0.0017	–0.6696 ±0.0940	9.1519 ±0.2393	–79.0660 ±0.0885

experiments using the TLS point cloud only were carried out. In the experiments, scan 1 was taken as reference. As expected, no solution could be obtained since the geometry of conjugate lines in scans 2 and 3 was insufficient (only parallel horizontal lines). More specifically, overlapping scans can slide along the lines' direction while maintaining their collinearity. The experiment was then repeated using scans 1 and 2 only, where an appropriate geometry is available; that is, two or more non-coplanar line segments are available. For this experiment, a solution was possible and the results are reported in Table 4. With the inclusion of the photogrammetrically reconstructed lines, all scans could be properly registered demonstrating the efficiency of the proposed procedure. The results are presented in Table 5.

A qualitative analysis of the results was carried out by plotting all the coregistered scans together. By visual inspection of the generated point cloud (Fig. 6), a satisfactory result could be observed. To perform a quantitative assessment of the proposed procedure, regions in the overlap area between the scans were manually selected for the computation of the average normal distance between conjugate surface elements. To compute the normal distance, one of the scans was represented by TIN patches and the other by points. Using minimum distance criteria, conjugate point-patch pairs were established. Then, the average normal distance between the scans' conjugate point-patch pairs were computed [17]. The obtained results for the normal distances for different planar patches in different directions are reported in Table 6. These values show the strength of the proposed methodology since we have reached six millimeters average normal distance over the various overlapping areas. This is a quite promising result especially if we take into an account the sampling distance of the terrestrial data which is close to two centimeters.

Fig. 6. Transformed point clouds superimposed together.

Table 6. Statistics of normal distance between scans' point-patch pairs.

Maximum distance	0.025 m
Average normal distance	0.006 m
Standard deviation	0.004 m

IV. Conclusion

The direct acquisition of 3D object information has widely expanded the use of TLS systems to satisfy the needs of several applications, for example, industrial documentation, cultural heritage conservation, civil engineering, virtual reality applications, and urban planning. The data acquisition using such systems is usually carried out from several observation stations to guarantee complete coverage of the object of interest. The major issue associated with the process of obtaining a 3D model from a TLS system is the registration of all the acquired scans, which are defined in the sensor's local coordinate system, into a global coordinate system. Such a task requires large overlap between the scans along with conjugate surface elements with adequate geometry for the recovery of the transformation parameters relating the scans. In this work, a method that overcomes such a limitation through the combination of photogrammetric data in the registration process was introduced. The utilization of photogrammetrically reconstructed features will guarantee strong tying between the different laser scans as long as appropriate registration geometry is available between the photogrammetric model and each of the laser scans. Therefore, using such a method, the overlap between scans can be completely eliminated. Also, appropriate primitives which can handle the irregular nature of the TLS point cloud were proposed. More specifically, linear features were utilized since they can be reliably extracted from both photogrammetric and TLS data. In addition, man-made objects are rich in linear features, making their use appropriate for several applications. In this paper, the linear features are represented by sets of non-conjugate points. A point-based

similarity measure, which can deal with non-conjugate points, was proposed. The non-correspondence of the selected points along the linear features is compensated for by artificially restricting their weight matrices along the line directions. The performance and feasibility of the proposed methodology has been evaluated from experimental results using simulated and real datasets.

Future work will focus on increasing the level of automation of the primitives' extraction and matching processes. For situations where linear features might not be available, the algorithm will be extended to allow for the utilization of conjugate planar patches between the TLS and photogrammetric data. The coregistration of airborne LiDAR and photogrammetric data and terrestrial laser scanning and image data will be investigated as well. Moreover, the utilization of the imagery for the assignment of RGB information to the TLS point cloud will be explored. Such task is facilitated by the introduced registration method that ensures the coalignment of the photogrammetric and TLS data to a common reference frame. The combined use of laser and photogrammetric data is valuable for the generation of realistic 3D textured models.

References

[1] R.R. Roderick and Y. Fujimoto, "Digital Processing of Dynamic Imagery for Photogrammetric Applications," *IEEE Trans. Instrum. Meas.,* vol. 33, no. 1, Mar. 1984, pp. 45-51.

[2] P.J. Besl and N.D. McKay, "A Method for Registration of 3-D Shapes," *IEEE Trans. Pattern Anal. Mach. Intell.*, vol. 14, no. 2, Feb. 1992, pp. 239-256.

[3] K. Bae and D. Lichti, "Automated Registration of Unorganised Point Clouds from Terrestrial Laser Scanners," *Int. Archives Photogrammetry, Remote Sens. Spatial Inf. Sci.*, vol. 35, part B5, July 2004, pp. 222-227.

[4] M. Fabris et al., "High Resolution Data From Laser Scanning and Digital Photogrammetry Terrestrial Methodologies. Test Site: An Architectural Surface," *Int. Archives Photogrammetry, Remote Sens. Spatial Inf. Sci.*, vol. 38, 3/W8, Sept. 2009, pp. 43-48.

[5] K. Al-Manasir and C. Fraser, "Registration of Terrestrial Laser Scanner Data Using Imagery," *Photogrammetric Record*, vol. 21, no. 115, 2006, pp. 255-268.

[6] P. Ronnholm et al. "Registration of Airborne Laser Scanning Point Cloud with Aerial Images Through Terrestrial Image Block," *Int. Archives Photogrammetry, Remote. Sens. Spatial Inf. Sci.*, vol. 37, part B1, July 2008, pp. 473-481.

[7] A. Habib et al., "Using Ground Based Laser Scanners to Establish the Orientation of Terrestrial Imagery," *Proc. Optical 3D Meas. Tech. VI,* vol. 1, Sept. 2002, pp. 306-314.

[8] F. Nex and F. Rinaudo, "New Integration Approach of Photogrammetric and LiDAR Techniques for Architectural Surveys," *Int. Archives Photogrammetry, Remote Sens. Spatial Inf. Sci.,* vol. 38, 3/W8, Sept. 2009, pp. 12-17.

[9] A. Habib and T. Schenk, "New Approach for Matching Surface from Laser Scanners and Optical Sensors," *Int. Archives of Photogrammetry, Remote Sens. Spatial Inf. Sci.*, vol. 32, 3/W14, Nov. 1999, pp. 55-61.

[10] E. Baltsavias, "A Comparison Between Photogrammetry and Laser Scanning," *ISPRS J. Photogrammetry, Remote Sens.,* vol. 54, no. 2/3, 1999, pp. 83-94.

[11] G. Vosselman et al., "Recognizing Structure in Laser Scanner Point Clouds," *Int. Archives Photogrammetry, Remote Sens. Spatial Inf. Sci.*, vol. 46, 8/W2, Oct. 2004, pp. 33-38.

[12] N. Meierhold and A. Schimch, "Referencing of Images to Laser Scanning Data Using Linear Features Extracted from Digital Images and Range Images," *Int. Archives Photogrammetry, Remote Sens. Spatial Inf. Sci.*, vol. 38, 3/W8, Sept. 2009, pp. 164-170.

[13] L. Brown, "A Survey of Image Registration Techniques," *ACM Comput. Surveys*, vol. 24, no. 4, 1992, pp. 325-376.

[14] A. Habib, M. Ghanma, and M. Tait, "Integration of LiDAR and Photogrammetry for Close Range Applications," *Int. Archives Photogrammetry, Remote Sens. Spatial Inf. Sci.,* vol. 35, Part B5, July 2004.

[15] A. Habib et al., "Integration of Photogrammetry and LiDAR Data in a Multi-primitive Triangulation," *Conf. American Soc. Photogrammetry Remote Sens.*, Tampa, Florida, May 7-11, 2007.

[16] E.M. Mikhail and F. Ackerman, *Observations and Least Squares*, New York: University Press of America, 1976.

[17] A. Habib et al., "Alternative Methodologies for the Internal Quality Control of Parallel LiDAR Strips," *IEEE Trans. Geosci. Remote Sens.*, vol. 48, part 1, pp. 221-236.

Erwan Renaudin received the MEng in geomatics engineering from Ecole Superieure des Geometres Topographes in Le Mans, France and the MSc in remote sensing from the University of Paris VI, France. He is currently working toward the PhD from the Department of Geomatics Engineering at the University of Calgary, Canada, and is a fellow of Alberta Innovates Technology Futures. He has been working for ten years in the industry of precision surveying, laser scanning, and GIS in European institutes, including CERN. His research interests are photogrammetry and POLInSAR for 3D modeling of forest structure for biomass estimation.

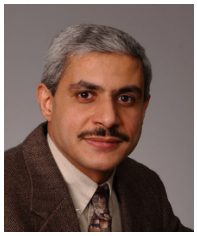

Ayman Habib, PEng, is a full professor and the head of the Geomatics Engineering Department at the University of Calgary. He holds a Bsc and an MSc in civil engineering from Cairo University, Egypt, and an MA and a PhD in geodetic science from the Ohio State University, USA. Dr. Habib's research interests include the fields of mobile mapping systems, calibration and stability analysis of low-cost off-the-shelf digital cameras, quality assurance and quality control of LiDAR systems, and multisensor data integration. He is a recent recipient of the Fairchild award from the American Society for Photogrammetry and Remote Sensing (ASPRS) for his long term contributions to photogrammetry.

Ana Paula Kersting received the BSc in civil engineering and the MSc in geodetic sciences from the Federal University of Parana, Brazil, in 2002 and 2006, respectively. Currently, she is a PhD candidate in the Digital Photogrammetry research group in the Department of Geomatics Engineering, University of Calgary, Canada. From 2002 to 2006, she worked as a GIS engineer for LACTEC – Institute of Technology for the Development, Brazil. Her research interests span the fields of terrestrial and aerial mobile mapping systems, multisensor data integration, quality assurance and quality control of LiDAR, and photogrammetric mapping.